
TOWARDS SCALABLE IOT DEPLOYMENT FOR VISUAL ANOMALY DETECTION VIA EFFICIENT COMPRESSION

Arianna Stropeni

University of Padova, Italy

arianna.stropeni@studenti.unipd.it

Francesco Borsatti

University of Padova, Italy

francesco.borsatti.1@phd.unipd.it

Manuel Barusco

University of Padova, Italy

manuel.barusco@phd.unipd.it

Davide Dalle Pezze

University of Padova, Italy

davide.dallepezze@unipd.it

Marco Fabris

University of Padova, Italy

marco.fabris.1@unipd.it

Gian Antonio Susto

University of Padova, Italy

gianantonio.susto@unipd.it

ABSTRACT

Visual Anomaly Detection (VAD) is a key task in industrial settings, where minimizing waste and operational costs is essential. Deploying deep learning models within Internet of Things (IoT) environments introduces specific challenges due to the limited computational power and bandwidth of edge devices. This study investigates how to perform VAD effectively under such constraints by leveraging compact and efficient processing strategies. We evaluate several data compression techniques, examining the trade-off between system latency and detection accuracy. Experiments on the MVTec AD benchmark demonstrate that significant compression can be achieved with minimal loss in anomaly detection performance compared to uncompressed data.

Keywords Visual Anomaly Detection · IoT · Feature Compression · Unsupervised Learning

1 Introduction

Visual anomaly detection (VAD) is essential in industrial automation for detecting defective parts via image-based inspection. Traditional VAD systems operate in centralized environments with high-performance computing and reliable data acquisition infrastructures [1]. However, with the rise of the Internet of Things (IoT), this paradigm is evolving. IoT enables distributed sensing for real-time asset monitoring across remote environments. Industrial IoT (IIoT) networks connect production sites, supporting flexible monitoring architectures [2, 3]. These changes introduce new constraints for VAD systems, as edge devices have limited resources and bandwidth, requiring the restructuring of VAD pipelines. This has spurred the development of lightweight, communication-efficient frameworks based on unsupervised deep learning and distributed processing [4].

VAD research spans from computer vision to deep learning, as documented in surveys [1]. Studies have explored anomaly detection under resource constraints [5]. Edge-assisted systems reduce latency in industrial monitoring [2], while [3] proposes low-latency VAD for smart cities. Research has also explored edge computing integration [4] and traffic flow analysis [6].

In IIoT, research has focused on communication resource allocation [7] and federated learning for distributed detection [8]. Studies have examined edge-cloud architecture trade-offs [9]. Optimization in VAD includes performance-aware

This work was partially carried out within the Italian National Center for Sustainable Mobility (MOST) and received funding from NextGenerationEU (Italian NRRP – CN00000023 - D.D. 1033 17/06/2022 - CUP C93C22002750006).

frameworks [10] and adaptive models [11]; whereas, the investigations on effective multi-objective methods aim to reduce latency and memory usage while maintaining accuracy [12].

While a universally accepted taxonomy of VAD methods is lacking, recent studies [13, 14] propose a classification into three main categories: reconstruction-based, synthesizing-based, and embedding-based approaches. Reconstruction-based methods assume anomalies cannot be reconstructed due to their absence in the training data (e.g., visual sensor networks in [15]); they use autoencoders, GANs, diffusion models, and Transformers to reconstruct normal samples, identifying anomalies via pixel-wise or SSIM-based differences. However, overfitting or visually similar anomalies can lead to missed detections. Synthesizing-based methods generate artificial anomalies on normal images, such as CutPaste [16] and DRÆM [17], but struggle to capture real-world defect variability. Finally, feature-based methods use pre-trained models to represent normal data distributions; examples include PaDiM [18], PatchCore [19], and FastFlow [20]. These methods achieve high accuracy but can be sensitive to domain shifts.

Nonetheless, to the best of our knowledge, the existing literature lacks solutions that jointly optimize VAD models and communication strategies for IoT. This paper proposes a lightweight, feature-based VAD framework for bandwidth-constrained IIoT environments, emphasizing efficient data transmission and interpretable anomaly localization. Our contributions are as follows:

- We propose a modular, resource-aware VAD pipeline for distributed edge-server deployment, optimizing detection performance, model footprint, and communication overhead for efficient anomaly detection in IoT environments.
- We investigate two strategies: image compression and lightweight CNN feature extraction with compression on the edge, reducing computational and communication burdens while preserving detection accuracy. Also, we explore compression techniques like WebP for image encoding, and random projection and product quantization for feature encoding, achieving high compression rates with minimal performance loss.
- We validate the framework using the MVTec AD dataset and MobileNetV2 as the edge feature extractor, showing that our method retains detection accuracy close to uncompressed data, suitable for real-world IIoT deployments.

The remainder of the manuscript unfolds as follows. Sec. 2 provides background on visual anomaly detection and formalizes the problem in an IoT context. Sec. 3 presents the proposed resource-aware VAD framework, describing both the system architecture and the methods for compressing features and images. Sec. 5 reports experimental results on the MVTec AD dataset, evaluating trade-offs between latency, bandwidth, and detection accuracy under various deployment scenarios. Finally, Sec. 6 concludes the paper and outlines directions for future research.

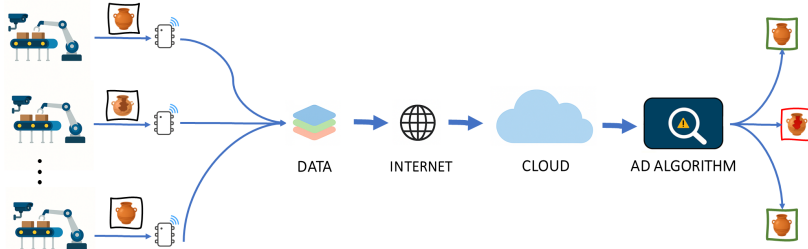


Figure 1: Overview of the VAD pipeline for IoT scenarios: edge devices acquire raw asset images and run compression techniques or apply feature extraction. Data are then sent across a bandwidth-limited IIoT channel to a central server. An anomaly detector (PatchCore in this study) is used to identify anomalous samples and localize defects.

2 Background and problem formulation

In the sequel, we provide the necessary background on VAD to formalize the optimization problem under analysis.

2.1 Mathematical preliminaries

We denote the set of CNN feature vectors as $\mathcal{F} = \{f_1, \dots, f_N\} \subset \mathbb{R}^d$, where each f_i is obtained by concatenating features from L intermediate layers at the same spatial location. A random subset $\mathcal{F}_s \subset \mathcal{F}$ is selected such that $|\mathcal{F}_s| = \alpha N$ with $\alpha \in (0, 1)$ denoting the sampling ratio.

For an input image x , the feature map at layer ℓ is denoted by $\phi^{(\ell)}(x) \in \mathbb{R}^{C_\ell \times H_\ell \times W_\ell}$.

The operator

$$\text{flatten} : \mathbb{R}^{C \times H \times W} \rightarrow \mathbb{R}^{CHW}$$

maps a 3D feature tensor to a vector.

The global image embedding is then constructed as

$$v = \text{concat}(f^{(1)}, f^{(2)}, f^{(3)}),$$

where concat denotes vector concatenation.

The vector $v \in \mathbb{R}^d$ is compressed using product quantization, denoted

$$\text{PQ} : \mathbb{R}^d \rightarrow \mathbb{R}^{d'} \quad (d' \ll d),$$

yielding the quantized representation $\hat{v} = \text{PQ}(v)$.

2.2 Visual anomaly detection approaches

This study focuses exclusively on feature-based methods, which offer a favorable trade-off between performance and computational cost. Feature-based VAD also enables localized detection and supports compact representations that are amenable to compression. Our previous work [5] demonstrated the viability of feature-based approaches in constrained settings. However, not all tasks can be performed at the edge due to computational limitations. IoT enables the use of more powerful anomaly detection models on the server, where computational and memory constraints are less restrictive. In addition, IoT facilitates the continuous updating of the anomaly detection model, a capability that is challenging to implement in fully edge-based solutions.

2.3 Problem formulation

We address the task of unsupervised visual anomaly detection (VAD) within an IoT-enabled industrial setting, where resource constraints on edge devices impose limitations on both computational capacity and communication bandwidth. The objective is to design a detection pipeline capable of operating across distributed nodes while minimizing data transmission costs and maintaining detection accuracy.

Let $\mathcal{X} = \{x_i\}_{i=1}^n$ denote a set of input images acquired by edge devices in an industrial IoT environment. Each image $x_i \in \mathbb{R}^{H \times W \times 3}$ must be analyzed for anomalies using an unsupervised visual anomaly detection (VAD) model. Let \mathcal{E} represent the set of edge devices, each subject to constraints on computational capacity and communication bandwidth.

Our goal is to learn a detection function

$$f : \mathbb{R}^{H \times W \times 3} \rightarrow \mathbb{R}, \quad f(x) \in [0, 1],$$

where $f(x)$ represents an anomaly score, with higher values indicating greater likelihood of abnormality.

The distributed nature of the system imposes two constraints:

- **Computation Constraint:** Each edge device $e \in \mathcal{E}$ has limited computational capacity, modeled as an upper bound C_e on permissible operations or model size.
- **Communication Constraint:** For each device e , the transmitted data $z_i = g(x_i)$ must satisfy $\|z_i\| \leq B_e$, where g is a compression or feature extraction function and B_e is the communication budget.

We aim to jointly design:

- a transmission function $g : \mathbb{R}^{H \times W \times 3} \rightarrow \mathbb{R}^d$ (either image compression or feature extraction),
- and a centralized detection model $f : \mathbb{R}^d \rightarrow [0, 1]$,

such that the expected anomaly detection performance is maximized:

$$\max_{f,g} \mathbb{E}_{x \sim \mathcal{X}} [\text{AUC}(f(g(x)))]$$

subject to the constraints:

$$\text{cost}(g; C_e) \leq C_e, \quad \|g(x)\| \leq B_e, \quad \forall x \in \mathcal{X}, e \in \mathcal{E}.$$

3 Proposed method

To address the problem of unsupervised visual anomaly detection (VAD) in IoT environments with limited computational and communication resources, we propose a distributed architecture consisting of two key components: edge devices and a centralized server. This architecture aims to balance computational load and communication costs while maintaining detection accuracy.

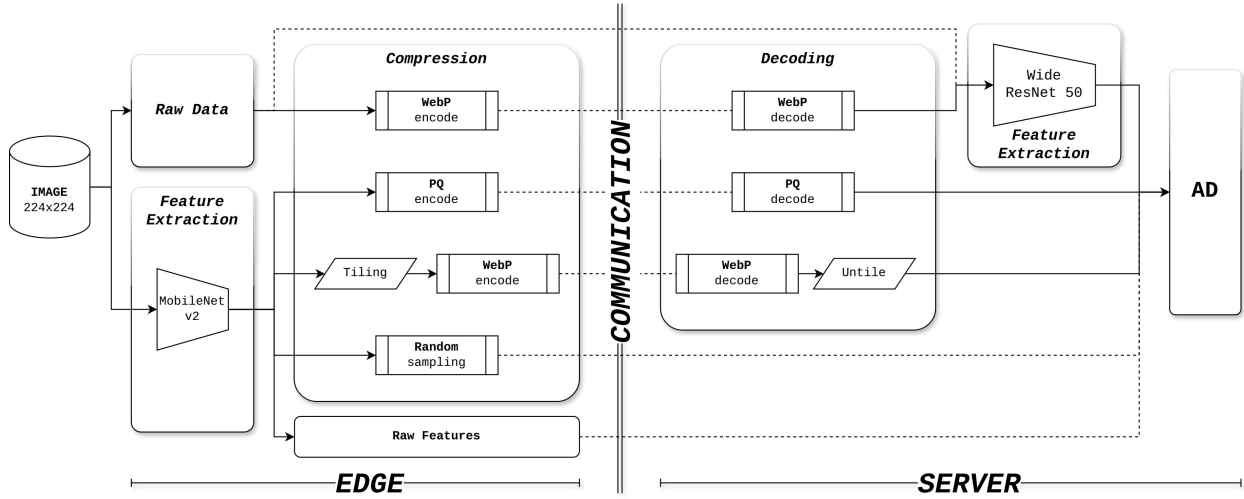


Figure 2: Illustration of the visual anomaly detection system architectures evaluated in this study. Different compression strategies are applied at the edge to raw data and features before transmission to the server for decoding and feature extraction.

The proposed pipeline is illustrated in Fig. 2. On the edge, the raw image data is first subjected to feature extraction via a lightweight convolutional neural network (CNN), such as MobileNetV2. Depending on the selected deployment strategy, this step is followed by either image compression or feature compression.

Once the compressed data reaches the server, the corresponding decoding operations are performed. For image compression, WebP decoding is applied, while for feature compression, PQ decoding is used. After decoding, the image or feature data undergoes a second feature extraction phase, typically using a more complex CNN like WideResNet50, to obtain embeddings suitable for anomaly detection. Finally, the processed data is passed through the anomaly detection (AD) module, which generates the anomaly score, indicating whether the input is anomalous or not.

This modular approach allows for flexibility in dealing with the trade-off between computational load on the edge and communication bandwidth requirements. In the following subsections, we will delve into each stage of this pipeline, examining the advantages and challenges associated with the various techniques employed.

3.1 Deployment architecture

To address computational heterogeneity and communication constraints in IoT environments, we propose a two-part distributed architecture. The core VAD model is hosted on a centralized server, while edge devices are responsible for either image acquisition and compression or feature extraction. We investigate two separate deployment strategies, each representing an alternative solution tailored to different resources and trade-offs:

1. **Image Compression at the Edge:** The device acquires an image, compresses it using standard codecs such as WebP, and transmits the compressed image to the server. This approach requires minimal memory overhead and implementation complexity, though encoding may be slower on CPU-bound devices.
2. **Feature Extraction at the Edge:** The device extracts intermediate features using a lightweight CNN (e.g., MobileNetV2), followed by feature compression. The resulting representation is then transmitted to the server. Although this strategy increases the memory footprint due to the model parameters, it reduces server-side processing and can be advantageous in fog computing scenarios.

3.2 VAD modeling and training

The VAD model is trained only on normal samples. At inference time, it must produce two outputs: (i) an image-level anomaly score indicating whether the entire image is anomalous or not, and (ii) a pixel-level anomaly map highlighting the spatial regions responsible for the anomaly. The latter enhances interpretability and allows human operators to assess the rationale behind a detection outcome.

3.3 Feature Compression Techniques

For the scenario involving on-device feature extraction, additional feature compression is applied to reduce communication overhead, considering the following strategies.

Random Sampling (RS): As adopted in several feature-based methods such as PaDiM [18], random sampling of feature maps significantly reduces dimensionality with minimal performance degradation, even at sampling factors of 0.25.

Let $\mathcal{F} = \{f_1, f_2, \dots, f_N\}$ denote the set of feature vectors extracted from N spatial locations across the output of L selected layers of a CNN (e.g., MobileNetV2). Each $f_i \in \mathbb{R}^d$ is the concatenation of features across the L layers at the corresponding spatial location. Random sampling selects a subset $\mathcal{F}_s \subset \mathcal{F}$ such that $|\mathcal{F}_s| = \alpha N$, where $\alpha \in (0, 1)$ is the sampling ratio.

Product Quantization (PQ). We apply product quantization [21] to compress the image embedding formed by concatenating the feature maps from a set of selected intermediate layers, referred to as feature extraction layers.

Let $L = \{1, 2, 3\}$ be the indices of the chosen feature extraction layers of the CNN. For a given input image x , let $\phi^{(\ell)}(x) \in \mathbb{R}^{C_\ell \times H_\ell \times W_\ell}$ denote the feature map output at layer $\ell \in L$.

Each feature map is flattened into a vector:

$$f^{(\ell)} = \text{flatten}(\phi^{(\ell)}(x)) \in \mathbb{R}^{C_\ell \cdot H_\ell \cdot W_\ell}$$

The image-level embedding is defined as the concatenation of all flattened feature maps from the selected layers:

$$v = \text{concat}(f^{(1)}, f^{(2)}, f^{(3)}) \in \mathbb{R}^d, \quad \text{with } d = \sum_{\ell \in L} C_\ell H_\ell W_\ell$$

This vector v is then compressed via product quantization:

$$\hat{v} = \text{PQ}(v),$$

and the quantized representation \hat{v} is transmitted to the server for anomaly detection.

Image-Based Compression of Feature Maps. As an alternative to PQ, we explore the use of a standard codec, specifically WebP, applied directly to intermediate feature maps as proposed by [22] for feature compression in object detection tasks.

The combination of lightweight CNNs and lossy but efficient compression mechanisms provides a viable solution for real-world IIoT applications, enabling high compression rates while preserving the interpretability and effectiveness of the anomaly detection process.

Table 1: Anomaly detection performance metrics comparison.

Methods		Original	Raw Features	WebP	RS	PQ	RS+WebP	RS+PQ
F1 pxl	objects	0.606	0.581	0.568	0.502	0.447	0.386	0.439
	textures	0.498	0.407	0.528	0.367	0.256	0.239	0.241
	overall	0.570	0.523	0.555	0.457	0.383	0.337	0.373
	overall $\Delta\%$	0.00%	-8.20%	-2.62%	-19.79%	-32.76%	-40.87%	-34.60%
ROC img	objects	0.979	0.977	0.976	0.950	0.877	0.877	0.870
	textures	0.995	0.956	0.992	0.927	0.700	0.771	0.661
	overall	0.984	0.970	0.982	0.942	0.818	0.842	0.800
	overall $\Delta\%$	0.00%	-1.43%	-0.28%	-4.29%	-16.94%	-14.47%	-18.73%

4 Experimental Settings

In this section, we evaluate the proposed VAD framework on IoT scenarios, describing the setup, transmission strategies, detection performance, and latency to highlight trade-offs between accuracy and efficiency.

4.1 Setting and data set

To evaluate the feasibility of deploying our method on resource-constrained edge devices, we compare inference times obtained on a high-performance server with estimated times for a typical edge device. All experiments were conducted using a single core of an AMD Ryzen Threadripper PRO 5995WX (128 cores) @ 2.7 GHz. To approximate the performance on an edge device, such as a Raspberry Pi-class processor operating at approximately 900 MHz, we scale the measured inference times by a factor of 3, corresponding to the ratio between the server and edge CPU clock frequencies (2.7 GHz / 0.9 GHz). This provides a coarse estimation of the latency expected on edge hardware under CPU-only execution.

For communication-related experiments, we assume a constant uplink bandwidth of 100 KBps per edge device, representing a typical constrained wireless link in practical IoT deployments. Communication latency and protocol overhead are assumed to be zero and are excluded from the scope of this analysis.

The MVTec AD Dataset [23] is an extensive repository of images designed specifically for evaluating AD algorithms. The MVTec AD includes ten object categories: Bottle, Cable, Capsule, Hazelnut, Transistor, Metal Nut, Pill, Screw, Toothbrush, and Zipper and five texture categories: Carpet, Grid, Leather, Tile, and Wood. Each category is provided with defect-free training images and annotated test images featuring a wide variety of anomalies (e.g., scratches, dents, contaminations) along with pixel ground-truth masks.

4.2 Examined scenarios

In this work, we evaluate various data transmission strategies within an IoT-based visual anomaly detection (VAD) framework. Each scenario reflects a different balance between compression rate, computational cost, and anomaly detection performance. We distinguish between two groups: *benchmark scenarios*, which are tested end-to-end for detection performance and system resource usage, and *scenarios with precomputed metrics*, where anomaly detection metrics are taken from previous work [5] and only computational requirements are newly evaluated.

All configurations are based on PatchCore [19] as the anomaly detection method, and all input images from the MVTec AD dataset [23] are uniformly resized to 224×224 . This resolution is standard in the VAD literature (e.g., PaDiM [18], CFA [24]) and is compatible with the input sizes of the MobileNetV2 and WideResNet backbones used in our experiments.

4.2.1 Benchmark scenarios.

- Feature Extraction with Random Sampling (0.25): The edge device extracts features using MobileNetV2, retains 25% of the patches via random sampling, and sends them to the server.
- Product Quantization (PQ): MobileNetV2-extracted features are compressed with PQ before transmission, and decoded on the server.
- Random Sampling (0.50) + PQ: Combines random sampling of MobileNetV2-extracted feature maps (50% retention) with PQ compression.
- Random Sampling (0.50) + WebP Compression on Feature Maps: Feature maps from each layer are tiled and compressed as an image using WebP as described by [22]. After transmission, the compressed image is converted back to feature tensors.
- WebP Compression (Quality 80) + Server-Side Feature Extraction: The image is WebP-compressed at the edge, then decoded and processed on the server using WideResNet.

4.2.2 Scenarios with precomputed metrics.

For the following settings, performance metrics have been sourced from our previous work [5], while timing and memory usage were profiled in this study.

- Raw Image Transmission (224×224): The downsampled image is sent directly to the server, where WideResNet performs feature extraction and anomaly detection.
- Raw Feature Transmission: Features are extracted on-device via MobileNetV2 and sent uncompressed to the server.

5 Results

5.1 Anomaly detection performance

We report the anomaly detection performance at both the image level and pixel level. Image-level performance is measured using the Area Under the ROC Curve (AUC), where the task is to classify whether an image contains any anomaly. Pixel-level performance is evaluated using the F1-score, where the model outputs a heatmap and each predicted pixel is compared against the corresponding ground truth pixel to assess segmentation accuracy.

Table 1 provides a comprehensive summary of the pixel-level (F1) and image-level (ROC AUC) scores, aggregated by objects, textures, and overall performance. In terms of pixel-level F1-score, WebP exhibits only a 2% drop from the baseline, followed by the MobileNetV2 edge feature extractor with an 8% loss. All other methods show significantly larger degradations, ranging from 20% to 40%, indicating poor localization accuracy. On the image-level ROC AUC metric, WebP again performs best, with only a 0.3% reduction from the baseline, while other methods suffer 16% to 20% drops. These results clearly highlight the advantage of using WebP compression for anomaly detection in IoT scenarios.

As shown in Figure 3, in terms of F1-scores, the WebP-based approach is the most consistent compression method in all object and texture categories from the MVTec benchmark. It achieves a performance nearly identical to that of sending the original uncompressed image, demonstrating that it preserves sufficient visual information for effective anomaly localization.

In contrast, the “raw features” method, which uses MobileNetV2 to extract features at the edge and transmits them directly, performs less consistently due to the constrained nature of the edge feature extractor. The WebP method instead transmits the compressed image to the server, where feature extraction is done with the more powerful Wide ResNet-50 backbone, resulting in better segmentation performance.

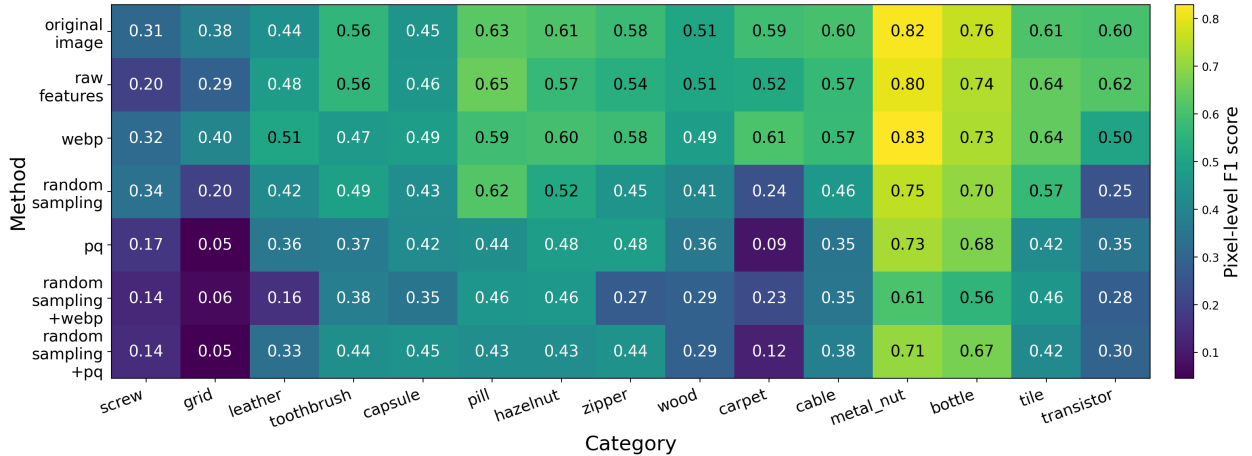


Figure 3: Pixel-level F1-scores across all MVTec categories.

5.2 Inference latency

The end-to-end inference latency is evaluated by accounting for edge-side feature extraction and optional compression, transmission over the fixed-bandwidth channel, server-side decoding, optional feature extraction, and anomaly detection using a KNN-based approach as in PatchCore.

Table 2 reports the latency breakdown for the main components of the pipeline: edge-side computation (either feature extraction, compression, or both) and server-side processing (which includes decompression, optional feature extraction, and anomaly detection inference).

As shown in Table 3, the method using WebP compression stands out in terms of end-to-end latency, thanks to the high efficiency of the codec. Additionally, hybrid strategies such as Random Sampling with Product Quantization (RS+PQ) and Random Sampling combined with WebP also achieve low latency, despite the additional cost of using a CNN-based feature extractor at the edge.

Table 2: Measured times for single image inference. All times are in milliseconds.

Method	Edge			Server	
	Feat. extract.	Encode	Decode	Feat. extract.	AD
Original	–	–	–	0.74	109.4
Features	15.0	–	–	–	105.7
RS.25	46.1	–	–	–	102.0
WebP	–	9.1	0.1	0.6	109.5
PQ	30.0	60.0	0.148	–	106.8
RS.5+PQ	30.0	17.7	0.102	–	103.8
RS.5+WebP	30.0	9.3	2.9	–	103.2

In contrast, transmitting raw features is prohibitively expensive under constrained bandwidth conditions, resulting in significantly higher total inference times.

The total times presented in Table 3 assume a fixed channel bandwidth of 100 kB/s, which is a realistic figure for Industrial Internet of Things (IIoT) applications. Although we plan to explore performance under varying bandwidths in future work, the current results already demonstrate substantial efficiency gains, achieving up to 80% reduction in end-to-end inference time, including edge processing, transmission, and server-side computation.

Table 3: **Comparison of image processing times across compression strategies.** Payload is the size (in kB) sent to the server. Tx Time is the transmission time over a 100 kB/s channel. Total Time includes edge, transmission, and server processing. Δ Time indicates total time change vs. baseline (Original). Lower is better for all metrics.

Method	Payload [kB]	Tx Time [s]	Total Time [s]	Δ Time
Original	60	0.60	0.71	0%
Raw Features	382	3.82	3.94	+455%
WebP	2	0.02	0.14	-80%
RS	95	0.95	1.10	+55%
PQ	4	0.04	0.24	-67%
RS + WebP	2	0.02	0.17	-76%
RS + PQ	2	0.02	0.17	-77%

5.3 Performance vs. Efficiency Trade-off

To better understand the trade-off between anomaly detection performance and communication efficiency, we combine the evaluation of pixel-level F1-score and transmitted payload size in a single scatter plot, shown in Figure 4.

Each point represents a method, positioned according to its pixel-level F1-score and the average payload size sent over the network. As expected, the WebP method lies closest to the ideal top-left region (high performance, low size), confirming it as the most effective compromise between accuracy and efficiency.

6 Conclusions and future directions

In this work, we proposed a modular and efficient visual anomaly detection (VAD) framework tailored for IoT scenarios, where resource constraints at the edge pose significant challenges. By investigating both image and feature compression strategies, we demonstrated that it is possible to significantly reduce communication overhead while preserving high anomaly detection accuracy. Our approach, validated on the MVTec AD dataset using a lightweight CNN and PatchCore as the detection model, achieves performance comparable to uncompressed pipelines, with reduced latency and memory requirements, making it suitable for practical industrial deployments.

Future research will explore dynamic adaptation strategies that adjust the compression method and level based on real-time constraints such as available bandwidth or computational load. Additionally, we plan to investigate learning-based feature compression techniques and extend the framework to support online model updates and real-time anomaly localization across heterogeneous edge-server systems.

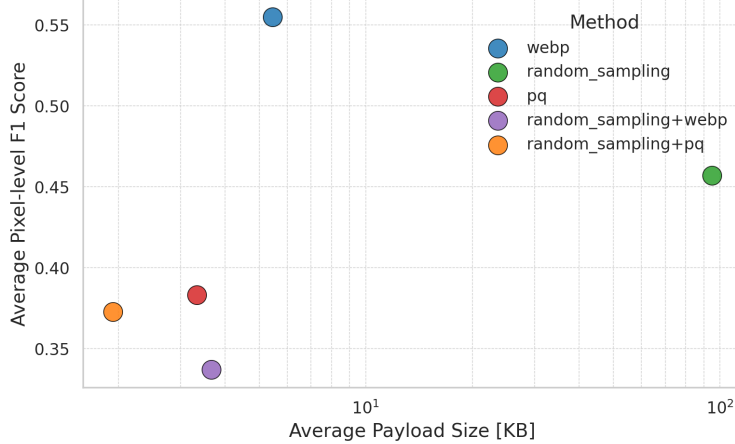


Figure 4: Trade-off between pixel-level F1-score and average payload size for each method.

References

- [1] J. Yang, R. Xu, Z. Qi, and Y. Shi, “Visual anomaly detection for images: A systematic survey,” *Procedia Computer Science*, vol. 199, pp. 471–478, 2022.
- [2] A. Chatterjee and B. S. Ahmed, “Iot anomaly detection methods and applications: A survey,” *Internet of Things*, vol. 19, p. 100568, 2022.
- [3] M. Fahim and A. Sillitti, “Anomaly detection, analysis and prediction techniques in iot environment: A systematic literature review,” *IEEE Access*, vol. 7, pp. 81 664–81 681, 2019.
- [4] B. Genge, P. Haller, and C. Enăchescu, “Anomaly detection in aging industrial internet of things,” *IEEE Access*, vol. 7, pp. 74 217–74 230, 2019.
- [5] M. Barusco, F. Borsatti, D. Dalle Pezze et al., “Paste: Improving the efficiency of visual anomaly detection at the edge,” *arXiv preprint arXiv:2410.11591*, 2024.
- [6] M. Fabris, R. Ceccato, and A. Zanella, “Efficient sensors selection for traffic flow monitoring: An overview of model-based techniques leveraging network observability,” *Sensors*, vol. 25, no. 5, p. 1416, 2025.
- [7] P. D. Rosero-Montalvo, Z. István et al., “Hybrid anomaly detection model on trusted iot devices,” *IEEE Internet of Things J.*, vol. 10, no. 12, pp. 10 959–10 969, 2023.
- [8] Y. Guo, T. Ji, Q. Wang et al., “Unsupervised anomaly detection in iot systems for smart cities,” *IEEE Tran. on Network Sci. and Eng.*, vol. 7, no. 4, pp. 2231–2242, 2020.
- [9] V. Mohindru and S. Singla, “A review of anomaly detection techniques using computer vision,” in *The Int. Conf. on Recent Innov. in Comp.* Springer, 2020, pp. 669–677.
- [10] G. F. Ceschini, N. Gatta, M. Venturini et al., “Optimization of statistical methodologies for anomaly detection in gas turbine dynamic time series,” *J. of Eng. for Gas Turbines and Power*, vol. 140, no. 3, p. 032401, 10 2017.
- [11] A. Gaurav et al., “Optimized trustworthy visual intelligence model for industrial marble surface anomaly detection,” *Alexandria Eng. J.*, vol. 118, pp. 503–511, 2025.
- [12] A. Durairaj et al., “Optimizing anomaly detection in 3d mri scans: The role of convlstm in medical image analysis,” *Applied Soft Computing*, vol. 164, p. 111919, 2024.
- [13] Z. Liu, Y. Zhou et al., “Simplenet: A simple network for image anomaly detection and localization,” in *Proceedings of the IEEE/CVF conf. on computer vision and pattern recognition*, 2023, pp. 20 402–20 411.
- [14] J. Quan, A. Tong et al., “Omni-ad: Learning to reconstruct global and local features for multi-class anomaly detection,” *arXiv preprint arXiv:2503.21125*, 2025.
- [15] L. Varotto et al., “Visual sensor network stimulation model identification via gaussian mixture model and deep embedded features,” *Eng. App. of A.I.*, vol. 114, p. 105096, 2022.
- [16] C.-L. Li, K. Sohn, J. Yoon, and T. Pfister, “Cutpaste: Self-supervised learning for anomaly detection and localization,” in *Proceedings of the IEEE/CVF conf. on computer vision and pattern recognition*, 2021, pp. 9664–9674.

- [17] V. Zavrtanik, M. Kristan, and D. Skočaj, “Draem-a discriminatively trained reconstruction embedding for surface anomaly detection,” in Proceedings of the IEEE/CVF Int. Conf. on computer vision, 2021, pp. 8330–8339.
- [18] T. Defard et al., “Padim: a patch distribution modeling framework for anomaly detection and localization,” in Int. Conf. on pattern recognition. Springer, 2021, pp. 475–489.
- [19] K. Roth, L. Pemula, J. Zepeda et al., “Towards total recall in industrial anomaly detection,” in Proceedings of the IEEE/CVF conf. on computer vision and pattern recognition, 2022, pp. 14 318–14 328.
- [20] J. Yu, Y. Zheng, X. Wang et al., “Fastflow: Unsupervised anomaly detection and localization via 2d normalizing flows,” arXiv preprint arXiv:2111.07677, 2021.
- [21] H. Jegou et al., “Product quantization for nearest neighbor search,” IEEE Tran. on pattern analysis and machine intelligence, vol. 33, no. 1, pp. 117–128, 2010.
- [22] H. Choi and I. V. Bajić, “Deep feature compression for collaborative object detection,” in 2018 25th IEEE Int. Conf. on Im. Processing (ICIP). IEEE, 2018, pp. 3743–3747.
- [23] P. Bergmann et al., “Mvttec ad—a comprehensive real-world dataset for unsupervised anomaly detection,” in Proceedings of the IEEE/CVF conf. on computer vision and pattern recognition, 2019, pp. 9592–9600.
- [24] S. Lee et al., “Cfa: Coupled-hypersphere-based feature adaptation for target-oriented anomaly localization,” IEEE Access, vol. 10, pp. 78 446–78 454, 2022.